Neoplasma 2022; 70(1): 58–70

doi:10.4149/neo_2022_220418N423

Zerumbone combined with gefitinib alleviates lung cancer cell growth through the AKT/STAT3/SLC7A11 axis

Jin-Guo WANG[1], Da-Lei LI[2], Rong FAN[3], Meng-Jun YAN[3,*]

[1]Department of Oncology, Yantai Hospital of Traditional Chinese Medicine, Yantai, Shandong, China; [2]School of Pharmacy, Key Laboratory of Molecular Pharmacology and Drug Evaluation Yantai University, Ministry of Education, Collaborative Innovation Center of Advanced Drug Delivery System and Biotech Drugs in Universities of Shandong, Yantai University, Yantai, Shandong, China; [3]Yantai Raphael Biotechnology Co., Ltd., Yantai, Shandong, China

**Correspondence: ymjchina1986@126.com*

Received April 18, 2022 / Accepted December 12, 2022

Zerumbone had been verified as a potential anti-cancer agent. Our research aimed to investigate the effect of zerumbone combined with gefitinib in lung cancer. Human pulmonary alveolar epithelial cells (HPAEpiC), A549, and H460 cell lines were used to detect the efficacy of zerumbone. BALB/c nude mice were randomly divided into five groups, including model, gefitinib (Gef, 10 mg/kg), low dose zerumbone (L-Zer, 20 mg/kg), high dose zerumbone (H-Zer, 40 mg/kg), and H-Zer + Gef groups, and the tumor growth in each group was monitored. TdT-mediated dUTP Nick-End Labeling (TUNEL) was used to detect cell apoptosis. Immunohistochemistry (IHC), immunofluorescence, and western blot were used to analyze the protein expressions in tumor tissues. Glutathione (GSH) and malondialdehyde (MAD) were detected by special kits. Zerumbone inhibited the proliferation of lung cancer cells in vitro. Tumor volume and weight were reduced after gefitinib or zerumbone treatment. Gefitinib and zerumbone treatment significantly promoted the apoptosis of tumor cells. The expression of Bcl-2, Bax, and P53 proteins confirmed cell apoptosis. IHC results indicated that zerumbone and gefitinib treatment decreased tumor angiogenesis. Consistent with this result, the expression of EGFR, VEGFR2, and Ki-67 proteins decreased, while the expression of angiostatin and endostatin proteins increased. Interestingly, zerumbone treatment increased the level of MDA while decreasing GSH. Next, the levels of glutathione peroxidase 4 (GPX4) and solute carrier family 7 member 11 (SLC7A11) decreased after zerumbone and gefitinib treatment. Our study suggested that zerumbone combined with gefitinib could effectively inhibit lung cancer for multi-model therapies, including the inhibition of tumor growth, angiogenesis, induce cell apoptosis, and ferroptosis.

Key words: tumor angiogenesis; cell apoptosis; EGFR; STAT3; ferroptosis

Lung cancer, as the leading cause of cancer-associated deaths among patients, has gained great attention [1]. Non-small cell lung cancer (NSCLC), which accounts for 80–85% of lung cancer cases, is the most common cancer [2, 3]. Radiation therapy, chemotherapy, and target therapy are eligible methods for NSCLC treatment [4, 5]. However, the overall five-year survival rate remained as before which accounted for less than 18% despite these advancements in lung cancer therapies [6].

Most NSCLC patients, who are often diagnosed in the intermediate and advanced period, missed the optimum opportunity for treatment. Systemic chemotherapy is the most important therapy for advanced NSCLC patients in which platinum-containing chemotherapy is the standard first-line treatment for NSCLC [7, 8]. Nevertheless, the toxic side effects of chemotherapy are various, which result in lower immune competence in the human body and affect the quality of life [9, 10]. In addition, the predecessors pointed out that NSCLC is less sensitive to traditional radiation therapy and chemotherapy in contrast to small cell lung cancer (SCLC) [11]. Therefore, NSCLC patients would experience unavoidable toxicity.

Gefitinib (Gef) is a small molecule EGFR tyrosine kinase inhibitor, which can benefit NSCLC patients with some EGFR mutations. Gef has a good inhibitory effect on EGFR mutant NSCLC cells, but the inhibitory effect on wild-type EGFR A549 cells is not ideal [12]. There is increasing evidence that traditional Chinese medicine and its active ingredients have good antitumor properties [13]. Zerumbone is mainly extracted from *Zingiber zerumbet* Smith. It has been verified that zerumbone is a potential anti-cancer agent, it could inhibit tumor cell proliferation and promote cell apoptosis [14, 15]. Previous studies provided evidence that zerumbone can suppress NSCLC via different mechanisms [16,

17]. However, the effect of zerumbone combined with Gef on NSCLC tumor growth remains unclear and the underlying mechanism is not well defined. In addition, the drug combination could reduce the single drug use concentration. Therefore, in this study, we first investigated the effect of zerumbone and Gef *in vitro*, then evaluated the efficacy of zerumbone combine Gef on tumor growth, analyzed the underlying mechanism related to apoptosis, angiogenesis, and ferroptosis in tumor xenograft mouse model.

Materials and methods

Cell culture. Human pulmonary alveolar epithelial cell (HPAEpiC) was purchased from the American Type Culture Collection (ATCC, USA) and cultured in the complete medium Dulbecco's modified Eagle medium/Nutrient Mixture F-12 (DMEM/F-12) (Thermo Fisher Scientific, USA) containing 10% fetal bovine serum (FBS, Gibco, USA). A549 and H460 cell lines were purchased from the Cell Bank of the Chinese Academy of Sciences, (Shanghai, China) was cultured in RPMI-1640 (SH30809.01, Hyclone, Shanghai, China) medium supplemented with 10% FBS. Cells were cultured regularly for reproduction. Cells were used to experiment in the logarithmic growth phase.

CCK-8 assay. 5×10^3 cells were seeded in 96-well plates. Following overnight incubation at 37 °C, the cells were treated with different concentrations of zerumbone (6.25, 12.5, 25, 50, and 100 μM, Z3902, Sigma-Aldrich, USA) or Gef (1.25, 2.5, 5, 10 and 20 μM, SML1657, Sigma-Aldrich, USA) for 24 h. NC group was treated with the same amount of dissolvent. Next, 10 μl of CCK-8 solution was added and incubated for 2 h at 37 °C. Then, the absorbance was measured at 450 nm using a microplate spectrophotometer (BioRad, USA).

Wound scratch healing assay. A549 and H460 cells were divided into four groups, including control, negative control (NC), Gef (15 μM), Zer (60 μM), and Zer + Gef groups. In brief, 1.5×10^5 cells were seeded into a 12-well culture plate. The wound was created using a 10 μl pipette tip after the cell density reached 100% confluency. At the start of the assay and following 24 h treatment, images were obtained using an optical microscope at ×200 magnification (Olympus, Japan). The migration ratio was calculated by ImageJ software (NIH, USA).

Transwell assay. A549 and H460 cells were resuspended at the concentration of 1×10^6 cells/ml with a serum-free medium. Then, 100 μl cells with different treatments were seeded into the upper chambers, while the lower chambers contained medium with 30% FBS cultured at 37 °C with 5% CO_2 for 48 h. Subsequently, the cells were stained with crystal violet and then observed under an optical microscope.

Animals and groups. A total of 45 male BALB/c nude mice (22.3±2.1 g) were purchased from Jinan Pengyue Experimental Animal Co., Ltd. (No. SYXK(Lu)20180030). Animals were maintained in standard steel wire cages under controlled conditions (temperature, 20–26 °C; humidity, 40–70%; lights, 12 h light/12 h dark cycle) with free access to food and water throughout the study. All animal procedures were carried out in accordance with the Guidelines of the Care and Use of Laboratory Animals (NIH Pub. No. 85-23, revised 1996) and have been approved by the Animals Ethics Committee of Yantai Raphael Biotechnology Co., Ltd.

The mice were injected with 1×10^7 cell/ml A549 cells (0.2 ml/mice) into the left axilla. Once the tumor volume reached 100 mm^3, the mice were randomly divided into 5 groups (n = 9/group): model (added vehicle), Gefitinib (Gef, 10 mg/kg), low dose zerumbone (L-Zer, 20 mg/kg), high dose zerumbone (H-Zer, 40 mg/kg), and H-Zer (40 mg/kg) + Gef (10 mg/kg) groups. The dose of zerumbone was based on the experience of hepatocarcinogenesis [18]. Drugs were obtained from Sigma-Aldrich (St. Louis, USA). Zerumbone or vehicle (5% DMSO in 10% Tween 80) and Gef were intraperitoneally injected once a day for 15 days. The tumor volume was observed every three days. After 21 days, mice were anesthetized with 0.3% sodium pentobarbital (45 mg/kg) and sacrificed by dislocating the cervical spine.

Tumor volume and tumor weight. The longest diameter (a) and the shortest diameter (b) of the tumor were determined every three days utilizing a vernier caliper. The tumor volume was calculated according to the following formula: $V=a\times b^2\times0.5$. After the mice were sacrificed, tumors were removed and weighed. A portion of the tumor tissue was embedded for IHC staining and TUNEL, another part was frozen in liquid nitrogen and stored at –80 °C for further analysis.

TdT-mediated dUTP Nick-End Labeling (TUNEL) assay. The embedded paraffin wax sections (4 μm) were dried, dewaxed, and hydrated with different levels of ethanol. Then, the sections were detected by the apoptosis detection kit (Beyotime, Shanghai, China). 5 fields of view were randomly selected to observe the apoptosis of tissue by the 200× optical microscope (Leica, Germany).

Immunohistochemical (IHC) assay. The embedded paraffin wax sections (5 μm) were dried, dewaxed, and hydrated with different levels of ethanol. Tissues were inactivated by 3% H_2O_2 methyl alcohol (80%) solution for 10 min, then heat-fixed for 10 min in citrate buffer (pH 6.0), and blocked with 5% bovine serum albumin (BSA, Beyotime, Shanghai, China) for 20 min. CD31 (ab28364, Abcam), EGFR (ab5652, Abcam), Ki-67 (ab15580, Abcam) antibodies were added and cultured at 4 °C for 12 h. Horseradish peroxidase-labeled goat anti-rabbit IgG (#7074, Cell Signaling Technology, USA). Color development of the sections used DAB (Solarbio, Beijing, China), and hematoxylin was used for counterstaining. The slices were dehydrated, transparent, and sealed. The slides were observed under a 200× optical microscope (Leica, Germany). The positively stained cells were counted using Image pro plus software (v6.0, Media Cybernetics, USA).

Microvascular density (MVD) analysis: According to the method of Weidner et al., the cytoplasm and nucleus

of tumor microvascular endothelial cells were stained with CD31 antibody. Isolated brown endothelial cells or clusters of endothelial cells were used as microvascular and counted. First, four areas with the densest vessels (dense hot spots) were selected under the 40× light microscope, and then the single and clustered endothelial stained cells were recorded as the observation area under the 400× light microscope, and the average value was taken as the microvessel density value [19].

Measurement of malondialdehyde (MDA) and glutathione (GSH). Tumor tissues were homogenized into a 10% tissue mixture, then the supernatant was obtained by centrifuging at 10,000 × g for 10 min at 4 °C. The level of MDA was detected by Lipid Peroxidation MDA Assay Kit (Beyotime, S0131, Shanghai, China), and GSH was measured according to the instructions (Beyotime, S0053, Shanghai, China).

Immunofluorescence double-labeling assay. To identify the distribution of SLC7A11 and GPX4 in tumor tissue, we incubated the sections with primary antibody against SLC7A11 (orb1150288, Biorbyt, UK) and GPX4 (sc166570, Santa Cruz, USA) overnight at 4 °C. Goat anti-rabbit IgG Cy3 and goat anti-mouse IgG FITC) were then added and incubated for 2 h. The signals were detected with the Leica SP8 Gated STED confocal microscope (Leica, Germany).

Western blot assay. The total protein of tumor tissue was extracted using radioimmunoprecipitation assay buffer (RIPA, Beyotime, Shanghai, China). A bicinchoninic acid assay (BCA) kit (Beyotime, Shanghai, China) was employed to determine the concentration of protein. 40 μg of proteins were separated with 10% sodium dodecyl sulfate-polyacrylamide gel electrophoresis (SDS-PAGE) and then transferred onto poly(1,1-difluoroethylene) membranes (PVDF, Millipore, USA). PVDF membranes were blocked with 5% skimmed milk at 4 °C overnight. Primary antibodies P53(1:500, ab26, Abcam), Bax (1:2000; ab32503, Abcam), Bcl-2(1:1000; ab32124, Abcam), p-Akt antibody (1:1000, #5012, Cell Signaling Technology, Boston, MA, USA), Akt antibody (1:1000, #9272, Cell Signaling Technology, Boston, MA, USA), p-STAT3 (1: 200; ab76315, Abcam); STAT3 (1:1000; ab31370, Abcam), VEGFR2 (1:1000; ab11939,

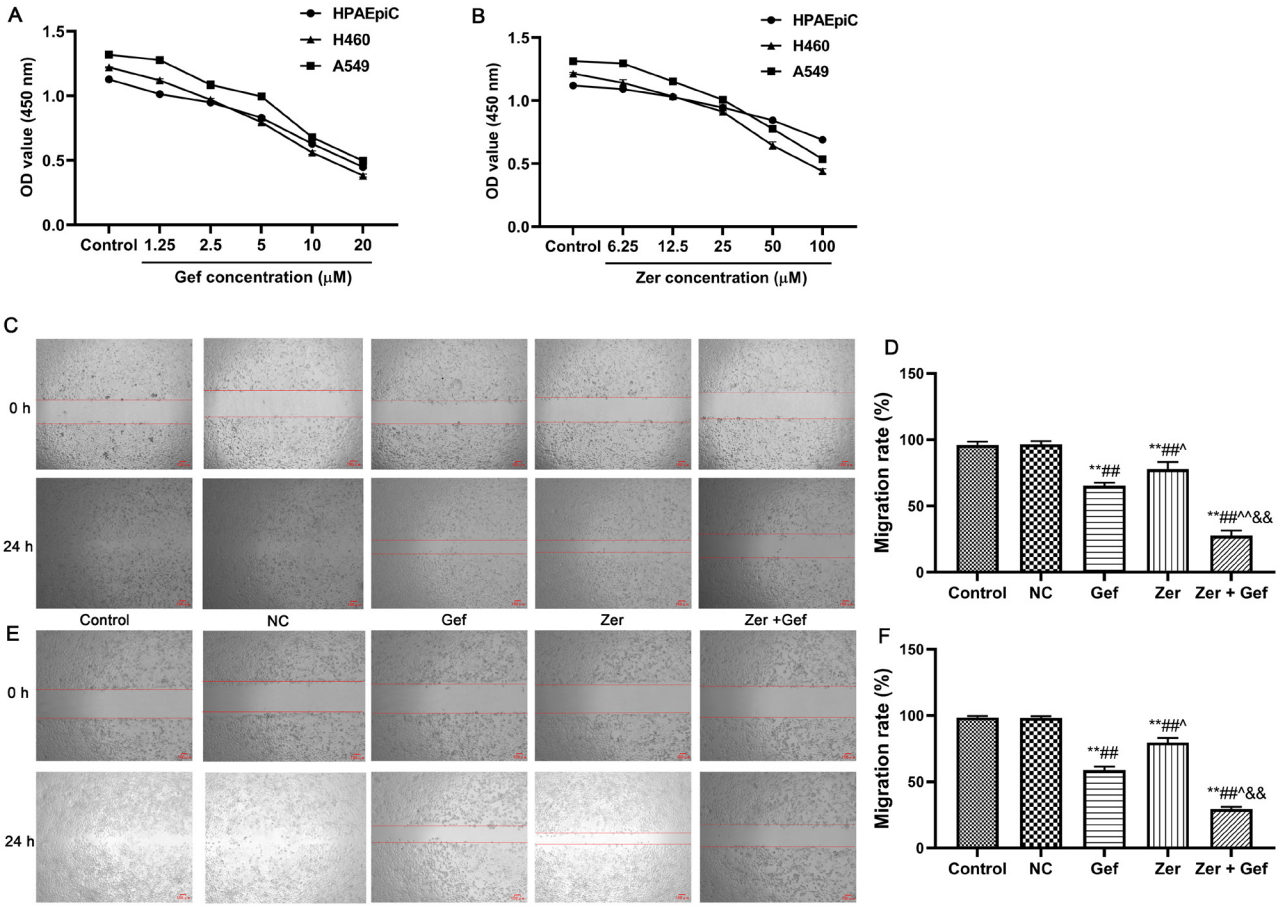

Figure 1. Zerumbone suppressed cell proliferation. A) The viability of A549 cells was detected by CCK-8 assay. B) The viability of H460 cells was detected by CCK-8 assay and the wound scratch healing assay was used to investigate the proliferation of A549 (scale bar: 100 μm) (C) and H460 (scale bar: 100 μm) (E) cells. The histogram presents the relative migration rate of A549 (D) and H460 cells (F). vs. control group, **p<0.01; vs. NC group, ##p<0.01; vs. Gef group, ^p<0.05, ^^p<0.01; vs. Zer group, &&p<0.01.

Abcam), angiostatin (1:2000; ab2904, Abcam), endostatin (1:500; ab202973, Abcam), EGFR(1:2000, ab52894, Abcam), GPX4 (1:2000, ab125066, Abcam), SLC7A11 (1:1000; ab216876, Abcam) were incubated at 4 °C overnight, then goat anti-rabbit IgG (1: 5000; ab205718; Abcam) or goat anti-mouse IgG (1: 5000; ab6789; Abcam) was incubated at 37 °C for 1 h. The protein bands were visualized by enhanced chemiluminescence (ECL) system (Thermo Fisher Scientific, Inc., USA). β-actin (1: 2000; ab8227; Abcam) was employed as an internal reference for the normalization of protein expression levels by ImageJ software (NIH, USA).

Statistical analysis. The statistical software SPSS 19.0 (SPSS Inc., Chicago, IL, USA) was used to analyze all data. Data are expressed as means ± SD. One-way ANOVA was used for the comparison of multiple groups followed by Tukey's post hoc test. A p-value <0.05 was regarded as statistically significant. All experiments above were repeated at least three times.

Results

Zerumbone combined with Gef inhibits cell proliferation. We investigated the effect of Zer and Gef on HPAEpiC, A549, and H460 cells. As presented in Figure 1, we first found that cell proliferation was suppressed after treatment with different dosages of Zer and Gef. However, Zer had little inhibitory effect on HPAEpiC but effectively inhibited A549 and H460 cells. Gef effectively inhibited HPAEpiC, A549, and H460 cells. Then we evaluated the effect of Zer and Gef on cell migration by wound scratch healing assay. The results showed that both Gef and Zer inhibited the migration of lung cancer cells, the effect of Zer combined with Gef was the most effective. The results of the Transwell assay were consistent with the wound scratch healing assay (Figure 2). In the further study, we evaluated the effect of Zer and Zer combined with Gef *in vivo*.

Zerumbone combined with Gef inhibits tumor growth in nude mice. In the tumor mice model, tumor volume (Figures 3A, 3B) and weight (Figure 3C) were significantly increased in the model group compared to different treatment groups ($p<0.05$). The tumor growth was significantly decreased in Gef, L-Zer, H-Zer, and H-Zer + Gef group ($p<0.05$). IHC staining of Ki-67, a widely used proliferation index [20], was investigated on tumor tissue. Notably, the results revealed that zerumbone combined with Gef significantly decreased the Ki-67 staining compared to the model group, zerumbone, or Gef treatment alone (Figures 3D, 3E; $p<0.05$). These results implicated that zerumbone could

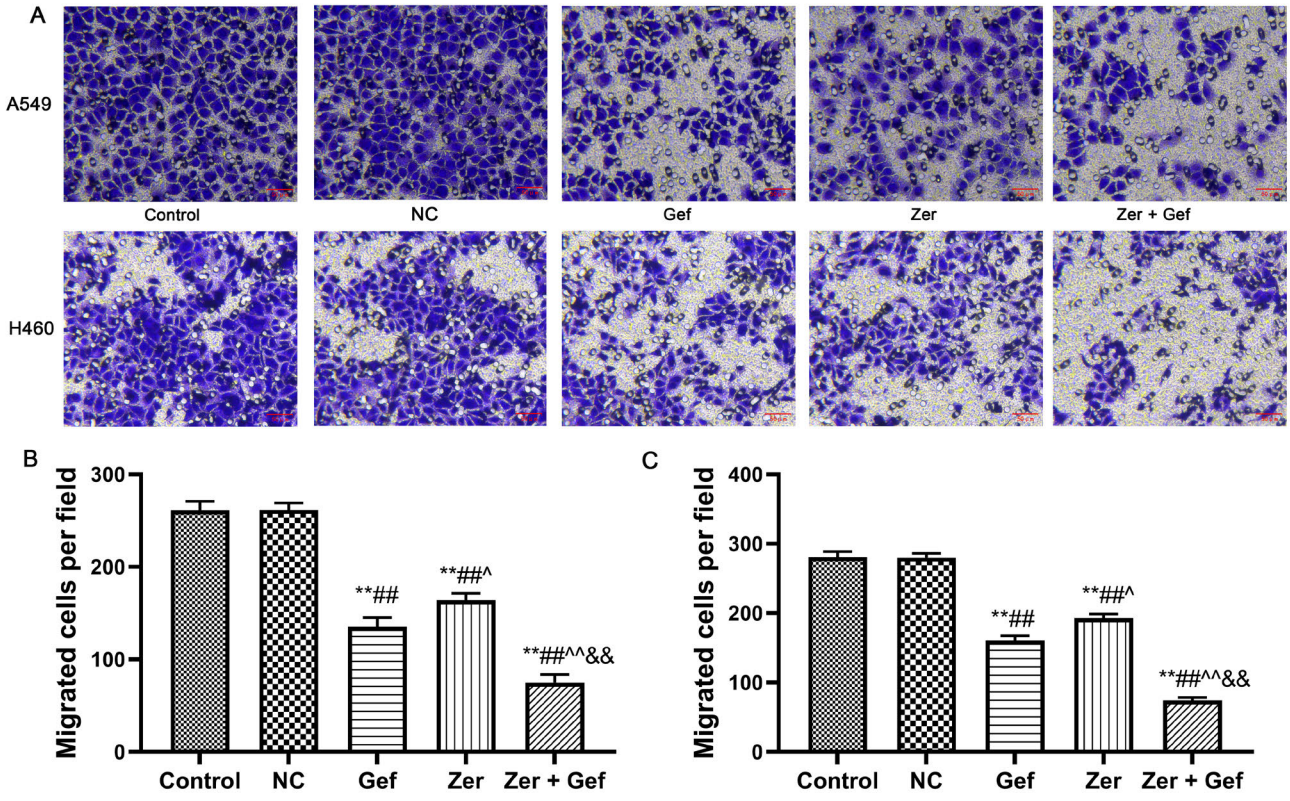

Figure 2. Zerumbone suppressed cell migration. A) Transwell assay was used to investigate the migration of A549 and H460 cells (scale bar: 50 μm). The histogram presents the migration of A549 cells (B) and H460 cells (C). vs. control group, **p<0.01; vs. NC group, ##p<0.01; vs. Gef group, ^p<0.05, ^^p<0.01; vs. Zer group, &&p<0.01.

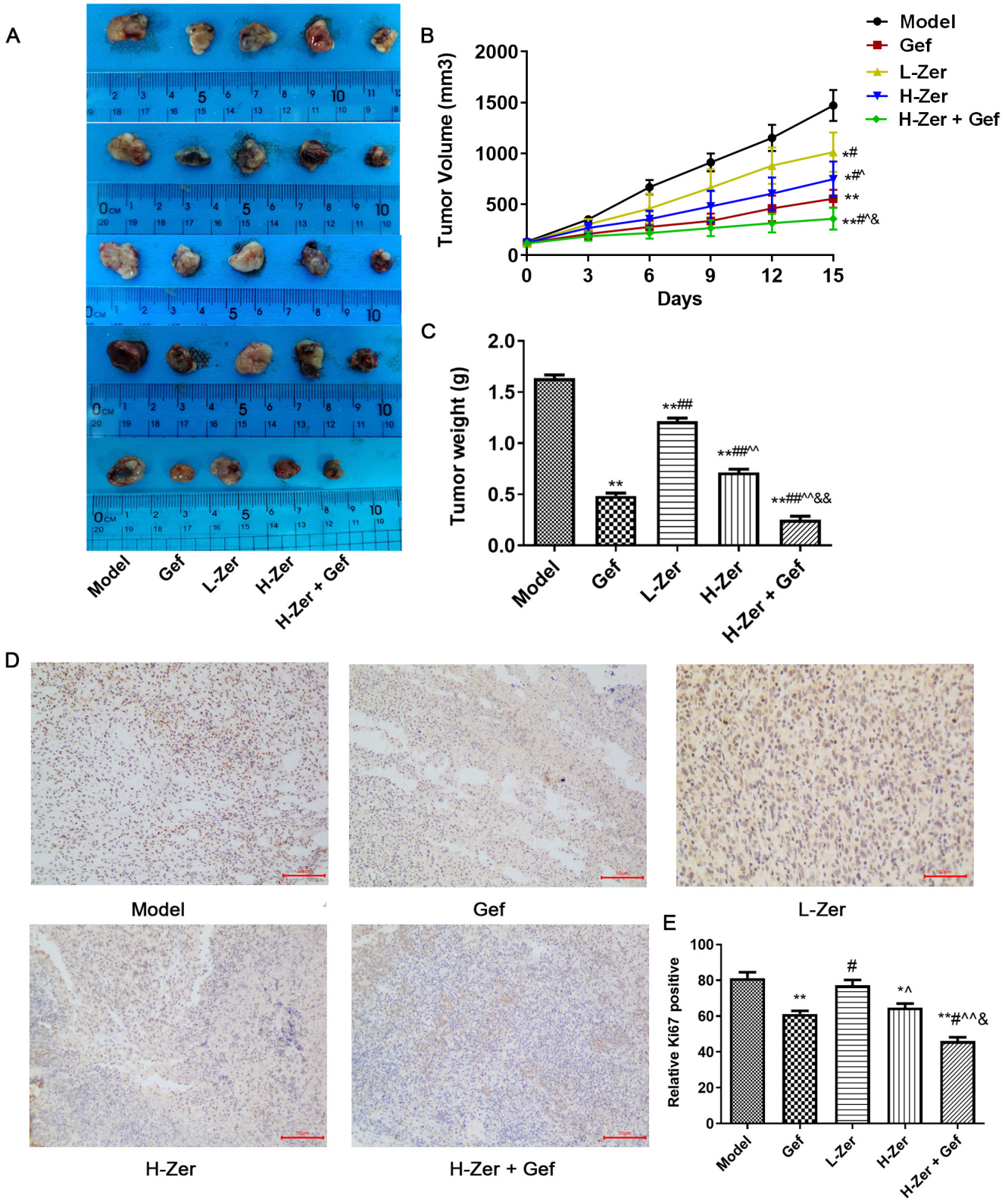

Figure 3. The effect of zerumbone or zerumbone co-treatment with Gef on tumor growth. A) Representative images of tumors; B) tumor volume; C) tumor weight. D) Ki-67 staining was investigated by IHC assay (scale bar: 50 μm). E) The positive percent of Ki-67. vs. model group, *p<0.05, **p<0.01; vs. Gef group, #p<0.05, ##p<0.01; vs. L-Zer group, ^p<0.05, ^^p<0.01; vs. H-Zer group, &p<0.05, &&p<0.01.

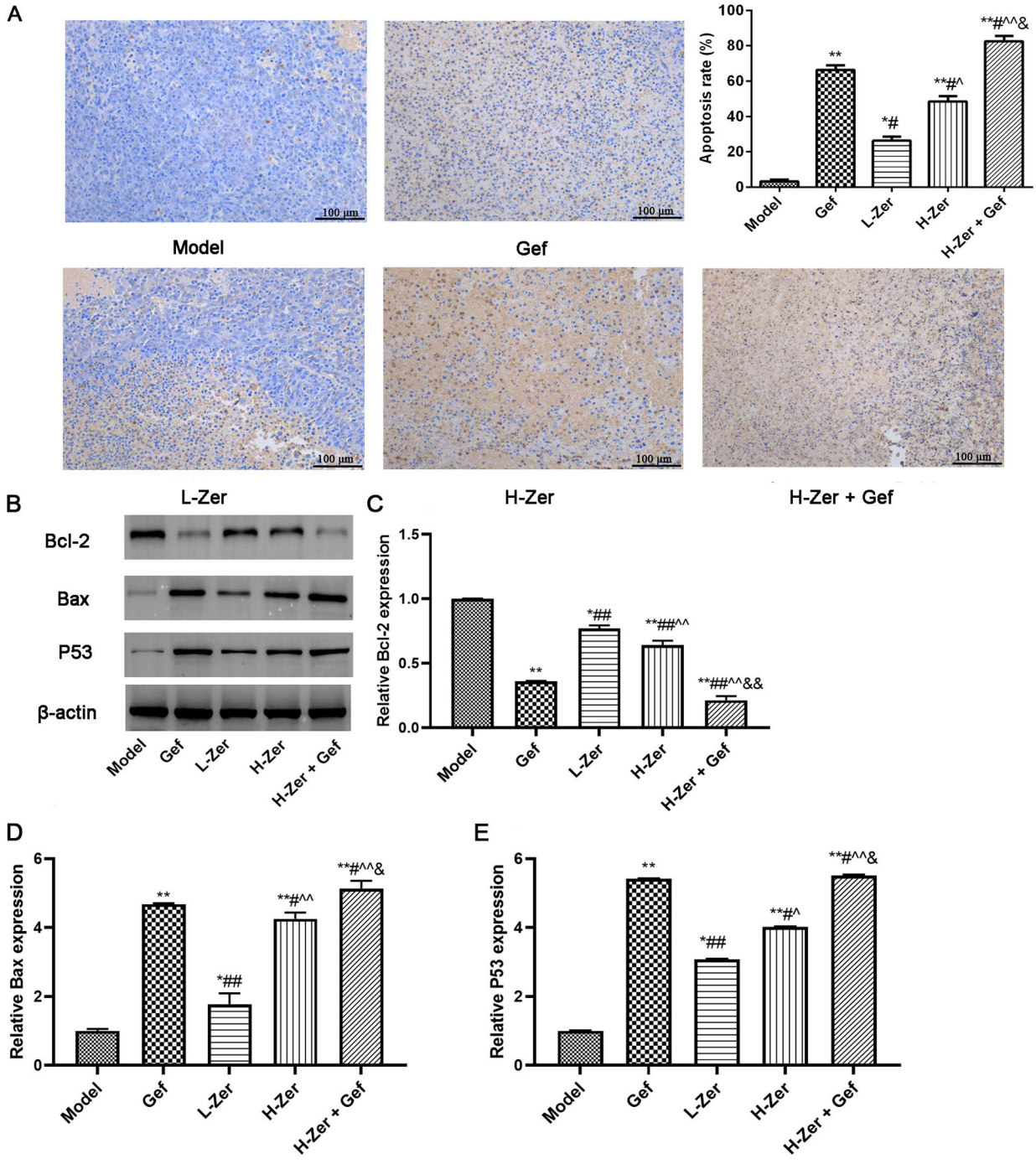

Figure 4. The effect of zerumbone or zerumbone co-treatment with Gef on apoptosis. A) The apoptosis of tumor cells was analyzed by TUNEL (scale bar: 100 μm). B) The expression levels of Bcl-2, Bax, and P53 were measured by a western blot. C) Relative expressions of Bcl-2 protein, D) Bax protein, E) P53 protein. vs. model group, *p<0.05, **p<0.01; vs. Gef group, #p<0.05, ##p<0.01; vs. L-Zer group, ^p<0.05, ^^p<0.01; vs. H-Zer group, &p<0.05, &&p<0.01.

suppress the progression of the tumor. The inhibitory effect of zerumbone combined with gefitinib was better than zerumbone or gefitinib treatment alone.

Zerumbone combined with Gef promotes apoptosis of tumor cells. The apoptosis of tumor cells was analyzed by TUNEL. Compared with other treatment groups, the number of apoptotic cells was the lowest in the model group, and the number of apoptotic cells was the highest in the Zer + Gef group (Figures 4A, 4B; p<0.05). Moreover, western blot results (Figure 4C) demonstrated that the expression

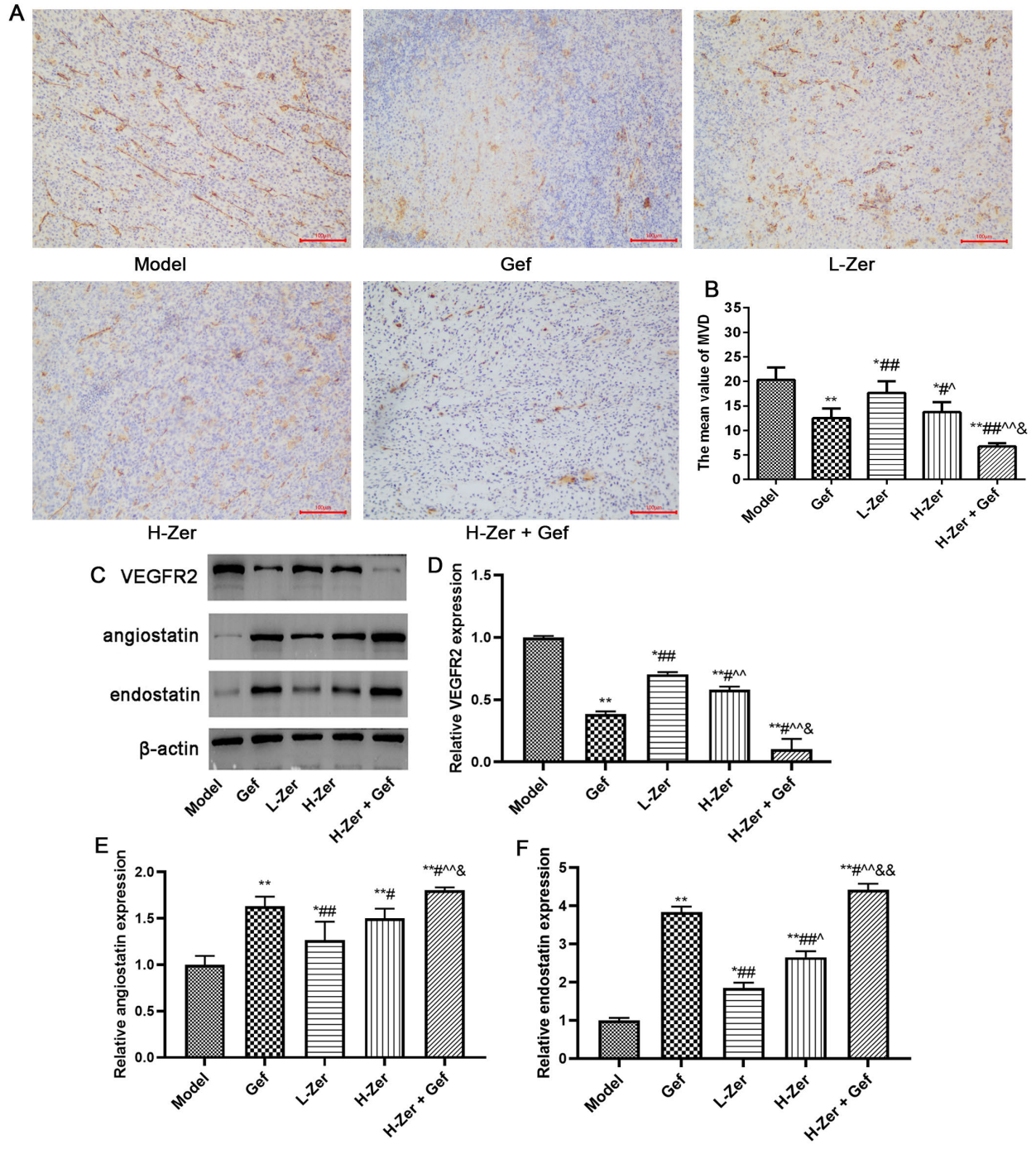

Figure 5. Zerumbone or zerumbone co-treatment with Gef inhibited tumor MVD. A) CD31 staining was investigated by IHC assay (scale bar: 100 μm). B) The mean value of MVD. C) The expression levels of VEGFR2, angiostatin, and endostatin were determined by a western blot. D) Relative expressions of VEGFR2 protein, E) angiostatin protein, F) endostatin protein. vs. model group, $^{*}p<0.05$, $^{**}p<0.01$; vs. Gef group, $^{\#}p<0.05$, $^{\#\#}p<0.01$; vs. L-Zer group, $^{\wedge}p<0.05$, $^{\wedge\wedge}p<0.01$; vs. H-Zer group, $^{\&}p<0.05$, $^{\&\&}p<0.01$.

of Bcl-2 protein in treatment groups significantly decreased compared to the model group, while the expression of Bax and P53 significantly increased (Figures 4D–4F; $p<0.05$).

Zerumbone combined with Gef decreases MVD in tumor tissues. Tumor angiogenesis is one of the common characteristics of solid tumors. When the volume of solid tumors exceeds 2 mm^3, angiogenesis must be involved, and it is closely related to tumor growth, invasion, and metastasis [21]. We investigated tumor MVD by CD31-staining. As presented in Figures 5A and B, the highest mean value

of MVD expression in the model group was 26.2±4.01, and those in the Gef, L-Zer, H-Zer, and H-Zer + Gef groups decreased to 9.88±1.44, 19.63±1.76, 13.12±1.35, and 6.73±1.36, respectively ($p<0.05$). The results demonstrated that zerumbone combined with Gef effectively inhibited tumor angiogenesis.

VEGFR2 plays a pivotal role in the development of the vascular system [22]. We detected the expression levels of VEGFR2, angiostatin, and endostatin protein. As shown in Figures 5C–5F, zerumbone and Gef treatment decreased the VEGFR2 expression while angiostatin and endostatin levels significantly increased ($p<0.05$). The results indicated that zerumbone and Gef treatment could attenuate tumor angiogenesis compared to the model group, zerumbone combined with Gef was more effective.

Zerumbone combined with Gef attenuated EGFR expression. We next explored the expression of EGFR by IHC. IHC result presented that zerumbone combined with Gef effectively decreased the expression of EGFR than zerumbone or Gef treatment alone (Figures 6A, 6B; $p<0.05$). The result of IHC was consistent with the western blot assay (Figure 6C).

Zerumbone combined with Gef decreased Akt and STAT3 expression in tumor tissues. To clarify the potential mechanism of the effect of zerumbone and Gef on tumor angiogenesis, a western blot assay was used to detect the expression of p-Akt and p-STAT3 (Figure 7). The results showed that zerumbone and Gef treatment decreased the expression levels of p-Akt and p-STAT3 compared with the model group. In addition, zerumbone combined with Gef

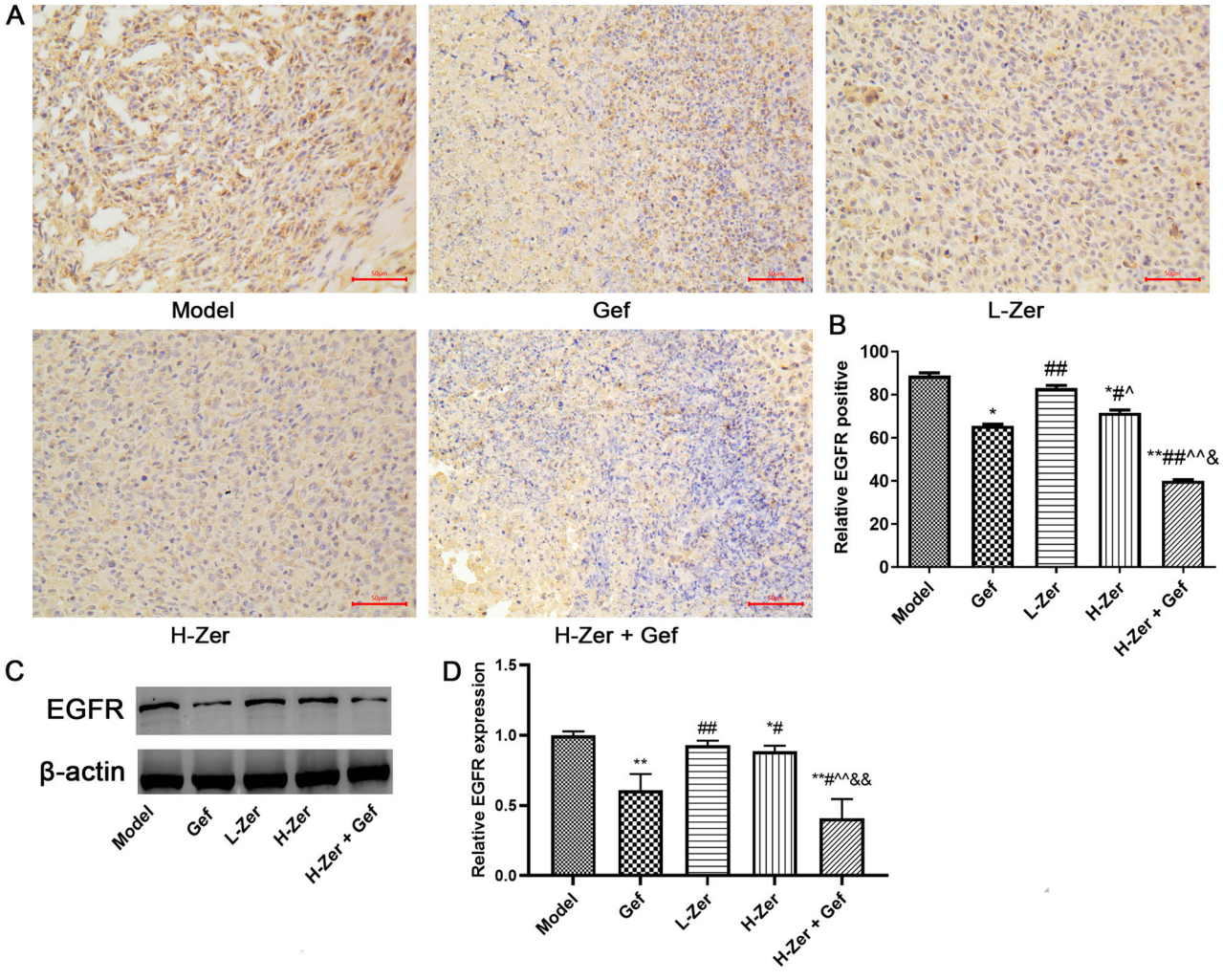

Figure 6. Zerumbone or zerumbone co-treatment with Gef inhibited EGFR in tumor tissues. A) IHC was performed to determine EGFR level (scale bar: 50 μm). B) The positive percentage of EGFR protein. C) Western blotting was performed to determine EGFR level. D) Relative expression of EGFR protein. vs. model group, *$p<0.05$, **$p<0.01$; vs. Gef group, #$p<0.05$, ##$p<0.01$; vs. L-Zer group, ^$p<0.05$, ^^$p<0.01$; vs. H-Zer group, &$p<0.05$, &&$p<0.01$.

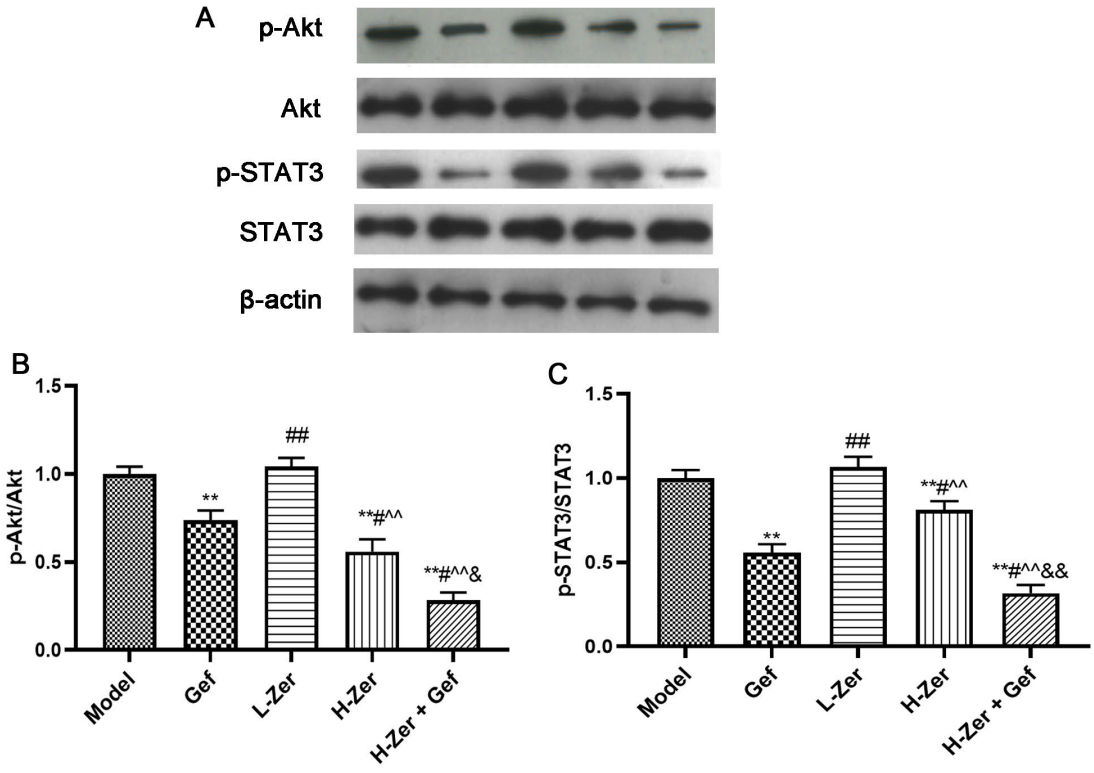

Figure 7. Zerumbone or zerumbone co-treatment with Gef inhibited Akt and STAT3 signaling. A) The expression levels of p-Akt, Akt, p-STAT3, and STAT3 were determined by a western blot. B) Relative expression of Akt; C) Relative expression of STAT3. vs. model group, $^{*}p<0.05$, $^{**}p<0.01$; vs. Gef group, $^{\#}p<0.05$, $^{\#\#}p<0.01$; vs. L-Zer group, $^{\wedge}p<0.05$, $^{\wedge\wedge}p<0.01$; vs. H-Zer group, $^{\&}p<0.05$, $^{\&\&}p<0.01$.

significantly decreased the expression of p-Akt and p-STAT3 ($p<0.05$) than zerumbone or Gef treatment alone.

Zerumbone combined with Gef induced cell death through ferroptosis in tumor tissues. To further investigate whether zerumbone induced cell death through ferroptosis, the levels of MDA and GSH were detected. In addition, ferroptosis-related proteins were examined by a double-labeling immunofluorescence assay and western blot. As presented in Figures 8A and 8B, the results presented that Gef and zerumbone treatment significantly increased the levels of MDA while diminishing the levels of GSH ($p<0.05$). Immunofluorescence double-labeling assay results presented that the expressions of SLC7A11 and GPX4 were localized in the cytoplasm (Figure 8C). Interestingly, the expression levels of SLC7A11 and GPX4 in different treatment groups decreased in tumor tissue. However, there was a significant difference between the H-Zer + Gef group compared with the model group ($p<0.05$). The result was consistent with the western blot (Figures 8D–8F).

Discussion

Gefitinib, a synthetic compound of small molecule phenylamine quinoline, is the first commercially available reversible epidermal growth factor receptor tyrosine kinase inhibitor (EGFR-TKI), which is applied to treat locally advanced or metastatic NSCLC [23]. Blocking the signal transduction pathway of EGFR, the inhibition of mitogen-activated protein kinase could lead to the apoptosis of tumor cells. In NSCLC patients, carcinoma proliferation is essential for tumor therapy. Previous research demonstrated that zerumbone was proven to be efficient to inhibit the proliferation of lung cancers via the FAK/AKT/ROCK pathway [17].

Previous studies suggested that zerumbone mediates the apoptosis of cancer cells by activating the P53 signal [16, 24]. In our study, we first investigated the effect of zerumbone or zerumbone combined with Gef on tumor growth, the results demonstrated that zerumbone combined with Gef could efficiently inhibit tumor volume and tumor weight. Furthermore, we found that zerumbone combined with Gef significantly decreased the Ki-67 staining. We then investigated the tumor cells' apoptosis by TUNEL. The results showed that zerumbone or Gef induced cell apoptosis. Furthermore, we detected the expression levels of P53, Bcl-2, and Bax. Our results demonstrated that the expression of Bax and P53 protein in the zerumbone and Gef treatment groups significantly enhanced, while the expression of Bcl-2 protein significantly attenuated. These results revealed that zerum-

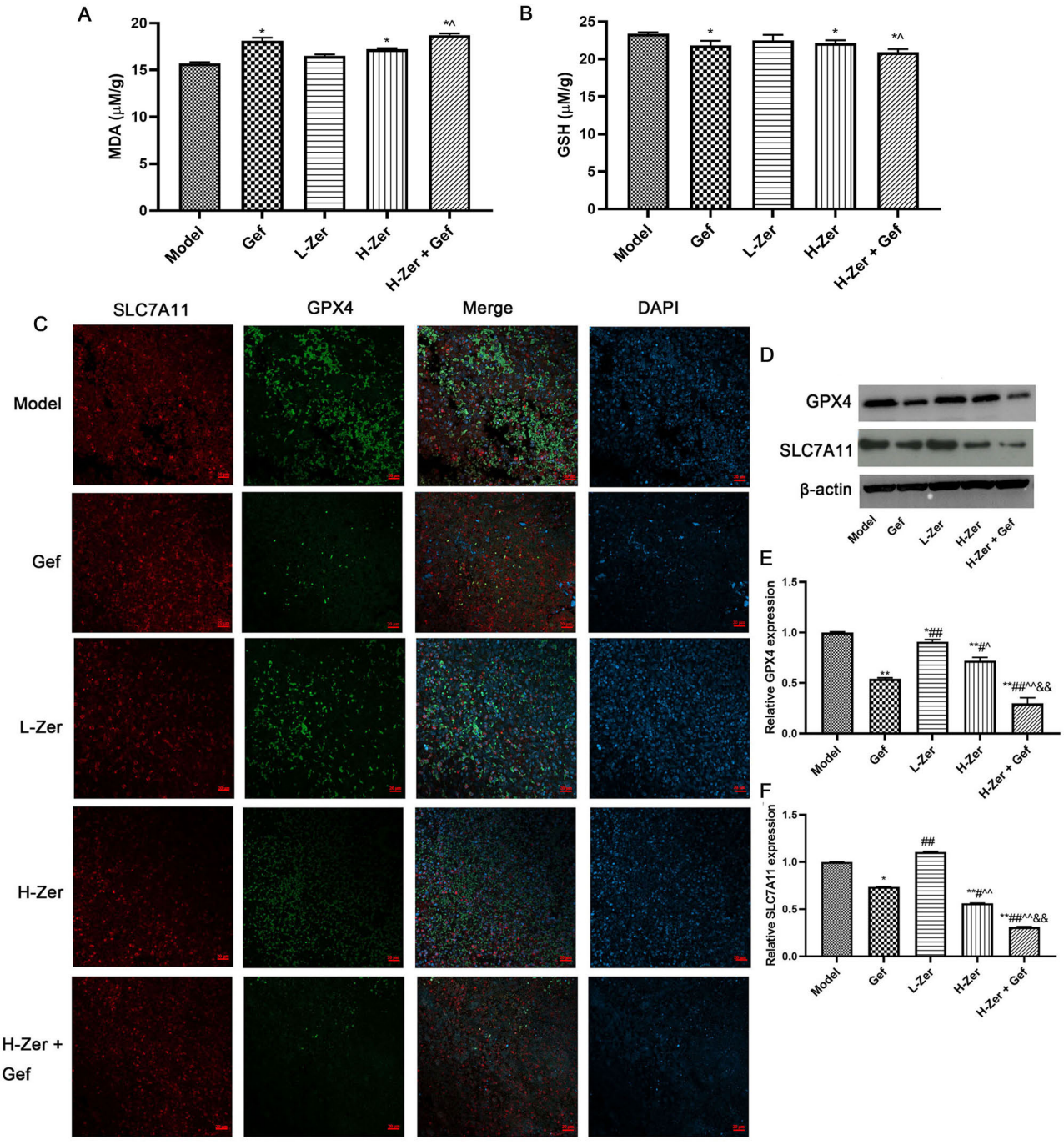

Figure 8. Zerumbone or zerumbone co-treatment with Gef promoted ferroptosis via diminished expression of SLC7A11 and GPX4. A) Zerumbone increased the level of MDA. B) Zerumbone decreased GSH content. C) Immunofluorescence double-labeling assay was used to locate the expression of SLC7A11 and GPX4 (scale bar: 20 μm). D) The expression levels of SLC7A11 and GPX4 were determined by western blot. E) Relative expression of SLC7A11. F) Relative expression of GPX4. vs. model group, *p<0.05, **p<0.01; vs. Gef group, #p<0.05, ##p<0.01; vs. L-Zer group, ^p<0.05, ^^p<0.01; vs. H-Zer group, &p<0.05, &&p<0.01.

bone could efficiently promote the apoptosis of NSCLC. Our results were consistent with previous studies [16, 24].

EGFR is closely related to the VEGFR signaling pathway. The high expression of VEGF leads to a large number of abnormal angiogenesis with abnormal structure and permeability, which promotes the abnormal proliferation of tumors. Interference with angiogenesis, mediated by the VEGF signaling pathway, can inhibit the invasion and metastasis of

tumor cells [25]. In addition, a previous study has shown that zerumbone could inhibit the proliferation of cholangiocarcinoma cells by targeting EGFR [26]. In the present study, we investigated tumor MVD by CD31 staining. The results of CD31 staining implied that zerumbone or Gef treatment decreased the expression level of CD31, and the mean value of MVD was the lowest after zerumbone combined with Gef treatment. Simultaneously, western blot results revealed that the expression levels of VEGFR2 and EGFR decreased, while angiostatin and endostatin expression levels increased. Angiostatin and endostatin are inhibiting factors of angiogenesis, the increasing level means the decreasing angiogenesis [27, 28]. Our results indicated that zerumbone could inhibit tumor angiogenesis, and zerumbone combined with gefitinib was more effective.

Akt is an important regulator and mediator for cell growth, proliferation, and apoptosis. The activation of the STAT3 signaling is significantly correlated with a poor prognosis and aggressive progression in lung cancer [29]. STAT3 signaling pathway has also been proven to be one of the pathways through which zerumbone downregulates the VEGF expression [30, 31]. In addition, zerumbone treatment inhibited cell biological activity in oral squamous cell carcinoma by suppressing the PI3K-mTOR signaling pathway, and the inhibition effect was associated with the suppression of Akt [32]. In our study, we also found that zerumbone could inhibit the phosphorylation activity of Akt and STAT3, and the results were consistent with previous studies [30–32].

Ferroptosis is an iron-dependent programmed cell death mode, which is different from apoptosis, cell necrosis, and autophagy. The main mechanism catalyzes the unsaturated fatty acids highly expressed on the cell membrane to produce lipid peroxidation and induce cell death [33]. In addition, it also shows the decrease of GPX4, the core enzyme regulated by the antioxidant system (glutathione system). Studies have shown that GPX4 knockout can enhance the sensitivity of triple-negative breast cancer cells to Gef by ferroptosis [34]. Accumulating evidence indicates that inhibition of SCL7A11 expression impairs GSH synthesis, resulting in severe oxidative stress [35]. In the current study, we detected the MDA and GSH content in tumor tissues. The results indicated that zerumbone combined with Gef could effectively decrease the level of GSH while increasing the level of MDA. Furthermore, the expression levels of SCL7A11 and GPX4 diminished in different treatment groups. The results indicated that the inhibition effect of zerumbone on tumors may be related to induced ferroptosis.

In summary, zerumbone could attenuate tumor growth by inducing cell apoptosis, inhibiting tumor angiogenesis, and maybe inducing ferroptosis. The putative underlying mechanism was associated with the inhibition of the AKT/STAT3/SCL7A11 axis. In addition, zerumbone combined with Gef was more effective. These findings implied that zerumbone is efficient for NSCLC therapy. On the basis of the above results, zerumbone may increase the sensitivity of A549 cells to Gef. Our study provides a novel sight into the treatment of NSCLC. However, our study only preliminarily detected the genes related to ferroptosis, the mechanism of zerumbone-inducing ferroptosis needs to be confirmed by more experiments in the future study. Furthermore, the effectiveness of zerumbone-increased the sensitivity of Gef needs a tremendous amount of clinical trials to verify.

References

[1] BILLATOS E, VICK JL, LENBURG ME, SPIRA AE. The Airway Transcriptome as a Biomarker for Early Lung Cancer Detection. Clin Cancer Res 2018; 24: 2984–2992. https://doi.org/10.1158/1078-0432.CCR-16-3187

[2] TANAKA F, YONEDA K. Adjuvant therapy following surgery in non-small cell lung cancer (NSCLC). Surg Today 2016; 46: 25–37. https://doi.org/10.1007/s00595-015-1174-7

[3] TSIM S, O'DOWD CA, MILROY R, DAVIDSON S. Staging of non-small cell lung cancer (NSCLC): a review. Respir Med 2010; 104: 1767–1774. https://doi.org/10.1016/j.rmed.2010.08.005

[4] DONOVAN EK, SWAMINATH A. Stereotactic body radiation therapy (SBRT) in the management of non-small-cell lung cancer: Clinical impact and patient perspectives. Lung Cancer (Auckl) 2018; 9: 13–23. https://doi.org/10.2147/LCTT.S129833

[5] HE X, ZHANG Y, MA Y, ZHOU T, ZHANG J et al. Optimal tumor shrinkage predicts long-term outcome in advanced nonsmall cell lung cancer (NSCLC) treated with target therapy: Result from 3 clinical trials of advanced NSCLC by 1 institution. Medicine (Baltimore) 2016; 95: e4176. https://doi.org/10.1097/MD.0000000000004176

[6] GLATZER M, ELICIN O, RAMELLA S, NESTLE U, PUTORA PM. Radio(chemo)therapy in locally advanced nonsmall cell lung cancer. Eur Respir Rev 2016; 25: 65–70. https://doi.org/10.1183/16000617.0053-2015

[7] RAMALINGAM S, BELANI C. Systemic chemotherapy for sdvanced non-small cell lung cancer: recent advances and future directions. Oncologist 2008; 13: 5–13. https://doi.org/10.1634/theoncologist.13-S1-5

[8] GOFFIN J, LACCHETTI C, ELLIS PM, UNC YC, EVANS WK. Lung Cancer Disease Site Group of Cancer Care Ontario's Program in Evidence-Based Care. First-line systemic chemotherapy in the treatment of advanced non-small cell lung cancer: a systematic review. J Thorac Oncol 2010; 5: 260–274. https://doi.org/10.1097/JTO.0b013e3181c6f035

[9] JU Y, HU Y, SUN S, WANG J, JIAO S. Toxicity and adverse effects of everolimus in the treatment of advanced nonsmall cell lung cancer pretreated with chemotherapy-Chinese experiences. Indian J Cancer 2015; 52: e32–e36. https://doi.org/10.4103/0019-509X.168954

[10] KANAT O, EVRENSEL T, BARAN I, COSKUN H, ZARIFOGLU M et al. Protective effect of amifostine against toxicity of paclitaxel and carboplatin in non-small cell lung cancer: a single center randomized study. Med Oncol 2003; 20: 237–245. https://doi.org/10.1385/MO:20:3:237

[11] KOMAKI R, SEIFERHELD W, CURRAN W, LANGER C, LEE JS et al. Sequential vs. concurrent chemotherapy and radiation therapy for inoperable non-small cell lung cancer (NSCLC): Analysis of failures in a phase III study (RTOG 9410). Lung Cancer 2000; 29: 93–93.

[12] ZHAO X, ZHANG N, HUANG Y, DOU X, PENG X et al. Lansoprazole alone or in combination with Gefitinib shows antitumor activity against non-small cell lung cancer A549 cells in vitro and in vivo. Front Cell Dev Biol 2021; 9: 655559. https://doi.org/10.3389/fcell.2021.655559

[13] YAO C, SU L, ZHANG F, ZHU X, ZHU Y et al. Thevebioside, the active ingredient of traditional Chinese medicine, promotes ubiquitin-mediated SRC-3 degradation to induce NSCLC cells apoptosis. Cancer Lett 2020; 493: 167–177. https://doi.org/10.1016/j.canlet.2020.08.011

[14] GIRISA S, SHABNAM B, MONISHA J, FAN L, HALIM CE et al. Potential of zerumbone as an anti-cancer agent. Molecules 2019; 24: 734. https://doi.org/10.3390/molecules24040734

[15] HAQUE MA, JANTAN I, ARSHAD L, BUKHARI SNA. Exploring the immunomodulatory and anticancer properties of zerumbone. Food Funct 2017; 8: 3410–3431. https://doi.org/10.1039/c7fo00595d

[16] HU Z, ZENG Q, ZHANG B, LIU H, WANG W. Promotion of p53 expression and reactive oxidative stress production is involved in zerumbone-induced cisplatin sensitization of non-small cell lung cancer cells. Biochimie 2014; 107: 257–262. https://doi.org/10.1016/j.biochi.2014.09.001

[17] KANG CG, LEE HJ, KIM SH, LEE EO. Zerumbone suppresses osteopontin-induced cell invasion through inhibiting the FAK/AKT/ROCK pathway in human non-small cell lung cancer A549 cells. J Nat Prod 2016; 79: 156–160. https://doi.org/10.1021/acs.jnatprod.5b00796

[18] WANI NA, ZHANG B, TENG KY, BARAJAS JM, MOTIWALA T et al. Reprograming of glucose metabolism by zerumbone suppresses hepatocarcinogenesis. Mol Cancer Res 2018; 16: 256–268. https://doi.org/10.1158/1541-7786.MCR-17-0304

[19] WEIDNER N, FOLKMAN J, POZZA F, BEVILACQUA P, ALLRED EN et al. Tumor angiogenesis: a new significant and independent prognostic indicator in early-stage breast carcinoma. J Natl Cancer Inst 1992; 84: 1875–1887. https://doi.org/10.1093/jnci/84.24.1875

[20] MILLER I, MIN M, YANG C, TIAN C, GOOKIN S et al. Ki67 is a graded rather than a binary marker of proliferation versus quiescence. Cell Rep 2018; 24: 1105–1112. https://doi.org/10.1016/j.celrep.2018.06.110

[21] ZHANG Y, ZHOU T, WANG H, CUI Z, CHENG F et al. Structural characterization and in vitro antitumor activity of an acidic polysaccharide from Angelica sinensis (Oliv.) Diels. Carbohydr Polym 2016; 147: 401–408. https://doi.org/10.1016/j.carbpol.2016.04.002

[22] SHALABY F, ROSSANT J, YAMAGUCHI TP, GERTSENSTEIN M, WU XF et al. Failure of blood-island formation and vasculogenesis in Flk-1-deficient mice. Nature 1995; 376: 62–66. https://doi.org/10.1038/376062a0

[23] MAEMONDO M, INOUE A, KOBAYASHI K, SUGAWARA S, OIZUMI S et al. North-East Japan Study Group. Gefitinib or chemotherapy for non-small-cell lung cancer with mutated EGFR. N Engl J Med 2010; 362: 2380–2388. https://doi.org/10.1056/NEJMoa0909530

[24] ABDELWAHAB SI, ABDUL AB, DEVI N, TAHA MM, AL-ZUBAIRI AS et al. Regression of cervical intraepithelial neoplasia by zerumbone in female Balb/c mice prenatally exposed to diethylstilboestrol: involvement of mitochondria-regulated apoptosis. Exp Toxicol Pathol 2010; 62: 461–469. https://doi.org/10.1016/j.etp.2009.06.005

[25] CHUNG TW, KIM SJ, CHOI HJ, KIM KJ, KIM MJ et al. Ganglioside GM3 inhibits VEGF/VEGFR-2-mediated angiogenesis: direct interaction of GM3 with VEGFR-2. Glycobiology 2009; 19: 229–239. https://doi.org/10.1093/glycob/cwn114

[26] SONGSIANG U, PITCHUANCHOM S, BOONYARAT C, HAHNVAJANAWONG C, YENJAI C. Cytotoxicity against cholangiocarcinoma cell lines of zerumbone derivatives. Eur J Med Chem 2010; 45: 3794–3802. https://doi.org/10.1016/j.ejmech.2010.05.029

[27] LI T, QIAN Y, ZHANG C, UCHINO J, PROVENCIO M et al. Anlotinib combined with gefitinib can significantly improve the proliferation of epidermal growth factor receptor-mutant advanced non-small cell lung cancer in vitro and in vivo. Transl Lung Cancer Res 2021; 10: 1873–1888. https://doi.org/10.21037/tlcr-21-192

[28] LIU W, YUAN R, HOU A, TAN S, LIU X et al. Ganoderma triterpenoids attenuate tumour angiogenesis in lung cancer tumour-bearing nude mice. Pharm Biol 2020; 58: 1061–1068. https://doi.org/10.1080/13880209.2020.1839111

[29] GRABNER B, SCHRAMEK D, MUELLER KM, MOLL HP, SVINKA J et al. Disruption of STAT3 signalling promotes KRAS-induced lung tumorigenesis. Nat Commun 2015; 6: 6285. https://doi.org/10.1038/ncomms7285

[30] JORVIG JE, CHAKRABORTY A. Zerumbone inhibits growth of hormone refractory prostate cancer cells by inhibiting JAK2/STAT3 pathway and increases paclitaxel sensitivity. Anticancer Drugs 2015; 26: 160–166. https://doi.org/10.1097/CAD.0000000000000171

[31] SHANMUGAM MK, RAJENDRAN P, LI F, KIM C, SIKKA S et al. Abrogation of STAT3 signaling cascade by zerumbone inhibits proliferation and induces apoptosis in renal cell carcinoma xenograft mouse model. Mol Carcinog 2015; 54: 971–985. https://doi.org/10.1002/mc.22166

[32] ZAINAL NS, GAN CP, LAU BF, YEE PS, TIONG KH et al. Zerumbone targets the CXCR4-RhoA and PI3K-mTOR signaling axis to reduce motility and proliferation of oral cancer cells. Phytomedicine 2018; 39: 33–41. https://doi.org/10.1016/j.phymed.2017.12.011

[33] JANG S, CHAPA-DUBOCQ XR, TYURINA YY, ST CROIX CM, KAPRALOV AA, TYURIN VA et al. Elucidating the contribution of mitochondrial glutathione to ferroptosis in cardiomyocytes. Redox Biol 2021; 45: 102021. https://doi.org/10.1016/j.redox.2021.102021

[34] SONG X, WANG X, LIU Z, YU Z. Role of GPX4-Mediated Ferroptosis in the Sensitivity of Triple Negative Breast Cancer Cells to Gefitinib. Front Oncol 2020; 10: 597434. https://doi.org/10.3389/fonc.2020.597434

[35] QIAN M, LOU Y, WANG Y, ZHANG M, JIANG Q et al. PICK1 deficiency exacerbates sepsis-associated acute lung injury and impairs glutathione synthesis via reduction of xCT. Free Radic Biol Med 2018; 118: 23–34. https://doi.org/10.1016/j.freeradbiomed.2018.02.028